

1       **DECISION SUPPORT IN HYPERSPECTRAL DATA ANALYSIS:**

2                   **A PROCEDURAL DESIGN AND A CASE STUDY**

3  
4                   Varun Madhok  
5                   Global Business Intelligence Solutions  
6                   IBM Canada Ltd.  
7                   3600 Steeles Avenue East  
8                   Markham ON L3S 9Z7, Canada  
9                   vmadhok@ca.ibm.com

10  
11                   David Landgrebe  
12                   School of Electrical & Computer Engineering  
13                   Purdue University  
14                   West Lafayette IN 47907-1285, U.S.A.  
15                   landgreb@ecn.purdue.edu  
16

17                   **ABSTRACT**

18           The distinguishing property of remotely sensed data is the multivariate  
19 information coupled with a two-dimensional pictorial representation. The analyst's  
20 interpretation of the image representation coupled with the spectral measurements on the  
21 pixel data is effectively a fusion of distinct data sources. This paper proposes remote  
22 sensing data analysis as a multi-source data fusion and presents a process model to guide  
23 the solution design. The paper illustrates the process with the analysis of airborne data  
24 collected over Washington D.C. in the generation of a detailed thematic map of the  
25 region.

26  
27           Key words: Hyperspectral data, masking, segmentation, digital elevation map,  
28 data fusion.

## 1. INTRODUCTION

The foundation of this paper is the proposition that effective multispectral image data analysis is an analyst driven placement of algorithms in which mathematical rigor, though of fundamental importance, is secondary to the analysis process design.

Multispectral remote sensing image data conveys information at the elemental level through the corresponding variations in the measured energy spectra, and at the composite level through the inter-pixel relationships. The subjective evaluations afforded by the image representation can be used as an interface between the human and the computer - thus supplementing mathematical analysis with the experience of the user analyst. This perspective can be developed into a procedural framework to initiate and guide the analysis of remote sensing data.

Section 2 of this paper discusses related research. It is claimed that the optimal engineering analysis is a data fusion where the human provides decision support in computer analysis. Section 2 proposes a process model substantiating this claim. Some guidelines for the design of a successful data analysis are presented. Section 3 executes the proposed strategy through a classification analysis of hyperspectral data collected for a flightline over Washington D.C.

## 2. INTERPRETING REMOTE SENSING DATA

If the input to the analysis is multispectral image data<sup>1</sup>, and the output is knowledge - the key to a successful extraction of knowledge from the data is information provided by the analyst. As an example, hyperspectral analysis [1] depends extensively on the insights obtained from the visual representation of the data in image form. In this context, the analyst is considered a source of data, and the process of analysis is a data fusion. The phrase 'data fusion' has been interpreted differently in different research. For

---

<sup>1</sup> By multispectral image data is meant data gathered over a scene on a pixel by pixel basis to constitute an image in which measurements are made for each pixel in a few to perhaps several hundred individual regions of the electromagnetic spectrum.

55 the present discussion, the definition by [2] is highlighted below as being of greatest  
56 relevance -

57 "... data fusion is a formal framework in which are expressed means and  
58 tools for the alliance of data originating from different sources".

59 It should be noted that the ensuing discussion does not attempt a design of  
60 learning/intelligent algorithms. The emphasis lies on the recognition of the human-  
61 computer interaction and the development of a synergy to utilize the strengths of the  
62 respective channels.

63

## 64 **2.1 Previous Work**

65 In the context of remote sensing analysis, data fusion is probably most commonly  
66 encountered as sensor fusion - the combination of data from various scanner-sources over  
67 a given scene. It is believed that merging data from different sensors makes the analysis  
68 robust against sensor noise and algorithmic deficiencies. This paper extrapolates the  
69 notion of sensor-source to include the analyst as an integral part of the analysis process.  
70 The philosophy of this approach is well described in a work by Kushnier, et al [4] in the  
71 context of military strategizing. The authors state that the task of making tactical  
72 decisions in naval operations is too complex to be accomplished by humans alone or by  
73 computers alone, and present several examples in support of the statement. The paper  
74 highlights the division of responsibilities between person and machine with the  
75 proposition that the human uses judgment and native intuition to make decisions while  
76 the assessment of the situational physics is a highly mathematical endeavor best left to  
77 the computer. Also of note is the work of McKeown, et al [5] for cartographic feature  
78 extraction. The methodology and the principles guiding the analysis are similar to those  
79 of the case study elaborated in Section 3.

80

## 81 **2.2 Principles of sensor fusion**

82 Mathematical modeling on the computer serves a useful purpose, in that the  
83 system dynamics can be reduced to the manipulation of a few parameters. If applicable,  
84 the complexity of the ensuing analysis can be significantly reduced, and thus be

85 synthesized by the user into a suite of analysis-routines. In contrast, the factor invaluable  
 86 to the successful application of laboratory models of terrestrial phenomena is the human  
 87 ability to learn and to adapt the analysis to the peculiarities of the problem. Successful  
 88 analysis is thus a balance between intuition and mathematics.

89 To maximize the benefit of human-machine interaction, this section identifies  
 90 some basic principles to guide analysis.

91

92 Axiom 2.1: Human abilities are different from those of the computer.

93 Consider Table 2.1 below, adapted from [6].

94

95 Table 2.1: The human versus the computer in data analysis.

96

The human	The computer
<ul style="list-style-type: none"> <li>· Can draw upon experience and adapt decisions to unusual phenomena.</li> <li>· Can reason inductively, and process hierarchically.</li> <li>· Can generalize from observations</li> <li>· Can generate output depending on subjective interpretation of task.</li> <li>· Is a source of data/information.</li> </ul>	<ul style="list-style-type: none"> <li>· Can perform repetitive pre-programmed actions.</li> <li>· Can process several items simultaneously.</li> <li>· Can implement the generalizations.</li> <li>· Generates output conforming to doctrines and performance indices based on a quantitative goal interpretation.</li> <li>· Has short response time, high speed of computation, and cheap data storage.</li> </ul>

97

98 The conclusion drawn from Table 2.1 is that the inferential aspects of the analysis  
 99 are best relegated to the human. The computer's abilities lie in the implementation of the  
 100 schemes (of analyst design).

101

102 Axiom 2.2: The machine (in)validates the user's hypothesis.

103 In various applications, the output of the algorithm is a measure of belief in the  
 104 hypothesis posed by the analyst. However, a poor output does not necessarily imply  
 105 algorithmic deficiencies. Failure can be a result of the performance index being  
 106 inadequate to the target task. An analysis is usually directed by the optimization of a user-

107 defined performance measure. Incompatibility between this measure and the objective is  
108 unlikely to produce the desired results. In regard to analyses that seek a visual  
109 interpretation of the data, this is an especially important (and often overlooked) issue.  
110 Algorithms that process data through the optimization of mathematical criteria are often  
111 sub-optimal in the sense that the output image is cluttered (or fuzzy or noisy) and is  
112 visually unpleasing.

113

114 Axiom 2.3: Every analysis requires at least one revision.

115 The current level of technology precludes the possibility of an intelligent system  
116 that operates independent of human input. Usually, analysis comprises various  
117 algorithmic 'objects', selected from a suite of procedures, linked in the appropriate  
118 sequence by the analyst. The optimal selection and ordering of these objects is often not  
119 known. Occasionally, algorithm parameterization is also dependent on human input. It  
120 may thus be concluded that almost any test run of the process is likely to produce results  
121 that can be improved upon through experimentation. The sub-text to Axiom 2.3 is that no  
122 practical engineering problem can be solved perfectly. The termination of analysis  
123 depends largely on the tolerance level for errors, the available resources, and the  
124 available time. It may also be inferred from Axiom 2.3 that, in the interest of effective  
125 time utilization, it is desirable to have the analysis output in a readily interpretable form.

126

127 Definition 2.4: Data fusion is an interface that allows collaboration among data sources to  
128 execute an analysis, enabling an assessment that is measurably superior to one in which  
129 the sources are incorporated singly.

130

131 The above definition is an enhancement to the proposition of [2] under the belief  
132 that definitions of the task and of the associated performance criterion are critical to the  
133 analysis process.

134

### 135 **2.3 A Process Model**

136 It is believed that any data analysis has to be designed to the peculiarities of the  
137 project at hand. In this sense, data analysis/mining/fusion is knowledge-based

138 engineering distinct from an algorithmic solution to a broad scientific problem. When  
139 designing such a data analysis project, the tasks can be divided into distinct modules that  
140 fundamentally remain unchanged, whatever the project objective. The process model of  
141 this section is an elaboration of these modules.

- 142 • TASK DEFINITION – We claim that every engineering problem can be designed to  
143 provide a useful solution provided the task is clearly defined and the measures of  
144 success are established at the onset. A rigorous task definition enables a judicious  
145 selection of the data sources, and a design of the analysis procedure. The measures of  
146 success limit the scope of the analysis.
- 147 • DATA SOURCES - The data sources, though restricted by availability, need to be  
148 assessed for their utility towards the task at hand, and for the presence of noise.  
149 Human interpretations and intervention are considered data sources essential to the  
150 process design. For instance, data sufficiently distinct from the general data  
151 population can alternately be considered outliers (noise) or data discoveries  
152 (information). The task of this module is to ensure the availability of adequate,  
153 appropriate and noise-free (within a user defined tolerance level) data for input to the  
154 analysis algorithms.
- 155 • DATA ANALYSIS – This module consists of a suite of algorithms required to perform  
156 analysis. Design considerations include procedural robustness and well-designed  
157 performance measures (Axiom 2.2).
- 158 • OUTPUT ASSESSMENT- The output of the analysis needs to be readily interpretable by  
159 the analyst (Axiom 2.1). A visually accessible output is especially desirable in remote  
160 sensing data analysis. The case study presented in the next section will demonstrate  
161 the value of image representations in remote sensing data analysis.
- 162 • TUNING - Finally, once the output has been assessed, the analyst proposes  
163 modifications (Axiom 2.3) and redoes the process.

164  
165  
166  
167  
168  
169  
170  
171  
172  
173  
174  
175  
176  
177  
178  
179

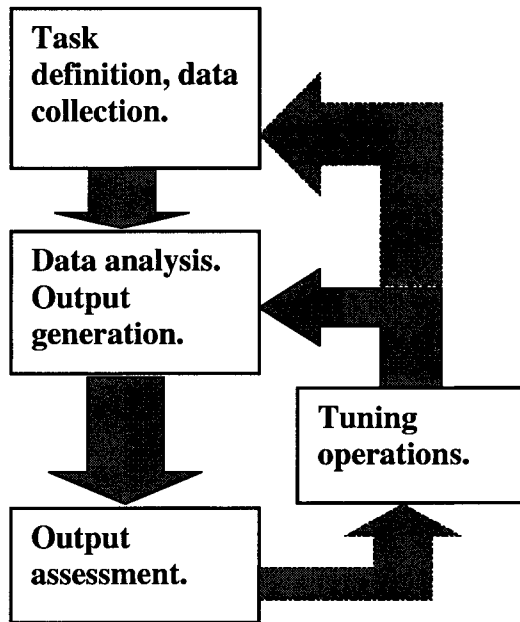


Fig. 2.1: Process model for data analysis.

180

### 3. A CASE STUDY - ANALYZING THE D.C. FLIGHTLINE

181 The HYDICE airborne scanner gathers data in each pixel over 210 channels  
182 (samples of the energy spectrum) between 0.4 and 2.4  $\mu\text{m}$ . The data for this case study  
183 was collected using the HYDICE scanner on a flightline over Washington D.C. The  
184 spatial representation of this data is a region 1310 pixels  $\times$  265 pixels. The spectral data  
185 measures the energy reflected from the Earth's surface. It is a standard assumption that  
186 these elemental spectral measurements contain the information from which the  
187 corresponding terrain-type or land-usage can be identified. Under the belief that the scene  
188 comprises a definite set of scene-classes (such as water, grass, trees, road etc.), the data  
189 are processed and each element (pixel) is assigned a label from the set of scene-classes. A  
190 color representation of the output is known as a thematic map or a classification map, the  
191 colors used in the representation being mapped one-to-one with the set of scene-classes.

192 The process model of Section 3.2 is invoked to frame the project design and its  
193 execution.

- 194 • TASK DEFINITION - The analysis requires the classification of the spectral data into a  
195 set of scene-classes that, to the extent of the analyst's belief, spans the thematic  
196 content of the data. For the given data, it is concluded that the thematic content of the  
197 data is spanned by the class-set {ROOF, ROAD, SHADOW, TREE, GRASS, WATER,  
198 PATH}. The criteria for task completion are the following - a subjective evaluation of  
199 the thematic map, an evaluation of the thematic map for 'picture quality' (absence of  
200 clutter, speckle noise), and a quantitative comparison of the classification against  
201 regions identified by an independent observer as specific scene-types.
- 202 • DATA SOURCES - The primary source of data, other than the analyst, is the HYDICE  
203 scanner. An additional source of information is the Digital Elevation Map (DEM) of  
204 the scene.
- 205 • DATA ANALYSIS - The various modules available for this analysis are discussed  
206 individually in Section 3.1 - The analysis suite.
- 207 • OUTPUT ASSESSMENT - The output at each iteration of the analysis is a thematic map  
208 produced using MultiSpec [8].
- 209 • TUNING - The tuning process is dependent on the stage at which the output is  
210 assessed. If the output is deemed deficient in a certain aspect, the analysis will be  
211 modified appropriately and re-done.

212 A sequential scheme of modular design will be used in the analysis. Each stage in  
213 the analysis will be referred to as a node in the process-sequence. Human-computer  
214 interaction will be emphasized through the analysis, and the analysis at each node will  
215 depend on the subjective assessment of the output at the previous node. The quantitative  
216 assessment of the analysis will be presented in the synopsis, Section 3.2.12.

217

### 218 **3.1 The Fusion Suite**

219 The essential terminology of this analysis report is defined below.

#### 220 **3.1.1 Thematic map**

221 The color two-dimensional composite of the classified data is known as a  
222 thematic map. The colors used in the representation being a one-to-one map from the set  
223 of scene-classes.

224



225 **3.1.2 Maximum likelihood classification**

226 The technique comprises the identification of training data - data representative of  
227 each of the classes in the set of scene-classes – followed by the construction of decision  
228 rules for the classification of the data. The analyst identifies a comprehensive set of  
229 scene-classes, and selects the training data. The algorithm assumes the spectral data are  
230 observations on parametrically describable processes whose parameters may be estimated  
231 using the training data. Mathematical details on the technique can be found in [9] [1] [3].  
232

233 **3.1.3 Unsupervised binary segmentation**

234 The unsupervised segmentation module used in this paper has been detailed in  
235 [7]. The input to the module comprises spectral data to be labeled from the set of scene  
236 classes, and the associated spatial locations of the data in the scene. The output is the  
237 labeling of the data into one of two scene classes. As an example, if a region in a scene is  
238 identified as vegetation, the technique can potentially separate the vegetation into two  
239 distinct categories – trees and lawn. The technique, as applied here, uses the masking  
240 scheme detailed in Section 3.1.6.

241

242 **3.1.4 Digital Elevation Map (DEM)**

243 The Digital Elevation Map of the scene is a two-dimensional pictorial  
244 representation of the scene elevation. The representation is quantitative for the computer  
245 and in shades of gray for the human. The lightness of a pixel's color is proportional to the  
246 elevation of the corresponding region in the scene. In Section 3.2.6, the DEM will be  
247 incorporated into the analysis to refine the identification of the rooftops in the flightline.  
248

248

249 **3.1.5 Decision tree (or graph) structure**

250 As per Axiom 2.3, it is believed that an acceptable solution does not take the form  
251 of a single algorithm. The optimal scheme for engineering a solution to the problem  
252 comprises an assessment-analysis cycle repeated as many times as desired. The analysis  
253 algorithm at each stage can be modified as per the assessment of the previous stage. If the  
254 process modules are laid out in order of their occurrence, the proposed solution takes the

255 form of a directed graph. A representation of the solution is shown at the end of Section 3  
256 in Figure 3.9.

257

### 258 **3.1.6 Masking**

259 Recall that the output of this analysis is to be a thematic map. At the end of each  
260 iteration of the analysis-assessment cycle, it may be discovered that data corresponding to  
261 some of the scene-classes have been accurately classified. This would correspond to  
262 certain regions in the scene that can now be spatially marked as distinct from the  
263 remainder of the data and excluded from further processing in the subsequent analysis-  
264 assessment cycles. A “masking” scheme excludes these data, and their labeling, from the  
265 scene. At the termination of the analysis on the unmasked data, the labels on the masked  
266 data can be recovered to complete the thematic map. Examples of the usage are in  
267 Section 3.2.3- Node 1 and Section 3.2.4 - Node 2.

268

### 269 **3.1.7 Negative training**

270 If the analyst has sufficient knowledge of the scene, he/she can conclude that a  
271 given scene-class is localized to a specific area. This implies that the set of scene-classes  
272 can be reduced outside the specified localization, and any data that are labeled from  
273 outside this reduced scene-class set need to be re-assigned labels. The ensuing analysis  
274 uses a simple re-labeling scheme - the scene-class of greatest frequency in the eight-point  
275 neighborhood of a given misclassified element is chosen as the new class-label. This  
276 process is termed "negative training", and its use has been illustrated in Section 3.2.7 -  
277 Node 5 and Section 3.2.8 - Nodes 6,7.

278

## 279 **3.2 D.C. Flightline Analysis**

### 280 **3.2.1 Data cleaning**

281 The 210 spectral channels<sup>2</sup> of data were individually examined for noise.  
282 Experience has shown that data can be corrupted for various reasons. Judgment on the  
283 data per spectral channel was made by visually examining the image representation for

284 the spectral response on each channel [8]. Histograms of some or all of the channels  
285 could also be constructed in order to look for additional types of distortion. Some causes  
286 for data corruption are listed below.

- 287 • Water absorption bands - an insufficient response over a given bandwidth. It can  
288 lead to an exaggerated sensitivity to sensor noise.
- 289 • Physical defects in scanner, such as scratches.
- 290 • Detector saturation due to unexpectedly light or dark scene objects.

291 Judgment on the analysis data was made by visually examining the output for  
292 each of the channels. In the present context, after excluding all such 'bad' data, 104  
293 channels remained of the original 210: Channels 55-100, 108, 113-132, 135, 152-164,  
294 173, 180-201. In the case of this data set, other types of distortion do exist, as is usually  
295 the case. As a result, it is desirable for the analysis algorithms to have a robustness such  
296 that such distortion have minimal negative effect.

297

### 298 **3.2.2 Root Node - Statistical analysis**

299 A three-color representation of the multispectral data using channels 60, 17 and  
300 27 (data gathered at wavelengths  $0.75\mu\text{m}$ ,  $0.46\mu\text{m}$  and  $0.5\mu\text{m}$  respectively) is shown in  
301 Figure 3.1.

302 The foundation of this study is statistical hyperspectral analysis, as developed and  
303 refined over the years by various researchers [9] [10] [1]. Fittingly, the output at this  
304 stage is called the Root Node. The analysis for this stage stepped through the following  
305 path.

- 306 • A comprehensive set of scene-classes was identified - {ROOF, ROAD, SHADOW,  
307 TREE, GRASS, WATER, PATH}.
- 308 • Training data representative of each of the scene-classes was selected.
- 309 • The Discriminant Analysis Feature Extraction technique [1][9] was used to reduce  
310 the dimensionality of the data on a class-conditional basis.
- 311 • The method of maximum likelihood classification was used to classify the  
312 spectral data to generate the thematic map.

---

<sup>2</sup>The channel number, as in this usage, signifies a specific wavelength at which the spectrum of energy reflected from the Earth has been sampled. Correspondingly, the 210 channels for the HYDICE scanner are representative of samples at 210 distinct wavelengths.

313           In the selection of training data representative of each of the classes, it was  
314 realized that some of the scene-classes (ROOF and ROAD) are a cumulative of several  
315 spectrally distinct sub-classes. Consequently, the set of scene-classes was enlarged to  
316 {ROOF1, ROOF2, ROOF3, ROOF4, ROOF5, ROOF6, ROOF7, ROOF8, ROAD1, ROAD2,  
317 SHADOW, TREE, GRASS, WATER, PATH}. Figure 3.3 is a representation of the associated  
318 training data. The results of the classification are shown as a thematic map in Figure 3.4.  
319 In Figures 3.4, note that the sub-classes of ROOF, and those of ROAD, have been merged  
320 into their respective groups. Subsequent representations of the output shall also not  
321 distinguish among the sub-classes. Sections of Figure 3.4 are enlarged as Figures 3.4b-e,  
322 to highlight the errors that need to be rectified in subsequent iterations of the analysis.



323

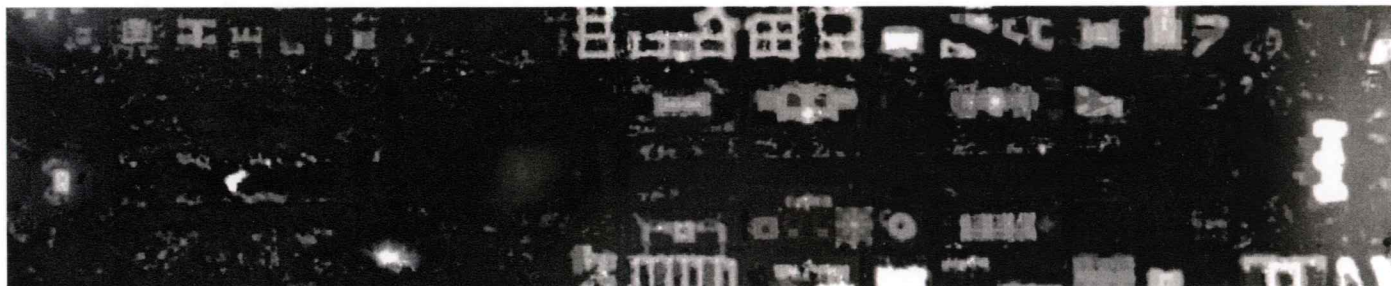
324

325

326

327

Fig. 3.1: Three-color simulated color IR film representation of D.C. flightline.



328

329

330

331

Fig. 3.2: Representation of the Digital Elevation Map. Note that the high elevation regions appear in a lighter shade of gray.

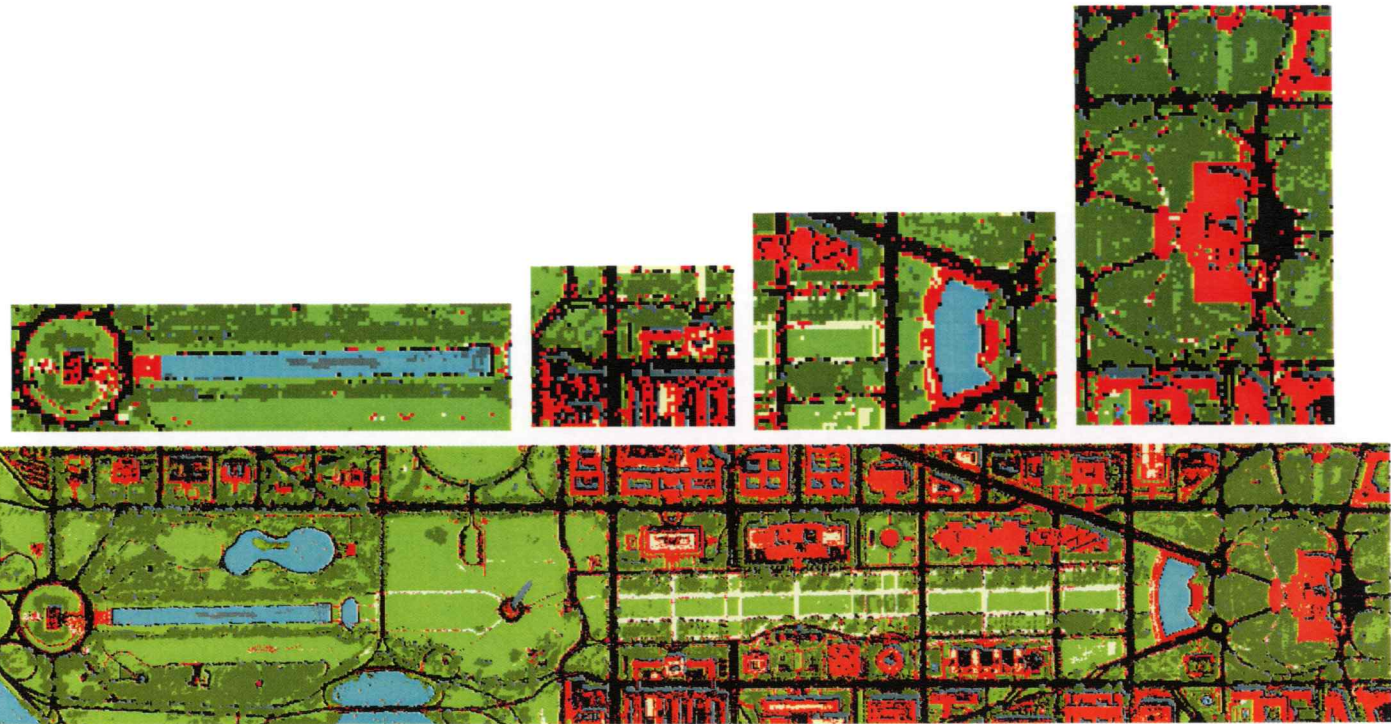
- Classes
- background
  - Roof1
  - Roof2
  - Roof3
  - Roof4
  - Roof5
  - Roof6
  - Roof7
  - Road
  - Road2
  - Path
  - Trees
  - Grass
  - Water
  - Shadow
  - Roof8



332  
333  
334  
335  
336

Fig. 3.3: Training data. Note that there are eight sub-classes to ROOF, and two sub-classes to ROAD.

337



338

339

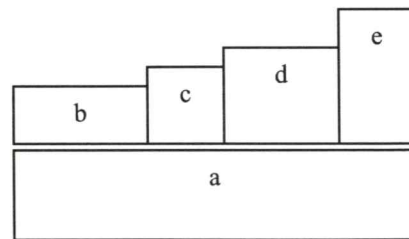


Fig. 3.4: a) The thematic map output from the maximum likelihood classification at the Root Node. b) Note that the analysis has identified 'SHADOW' in a water body. c) Note that clutter from ROAD and SHADOW corrupts ROOF identification. d) Note that class PATH clutters the middle of a lawn. e) Upon comparison with Figure 3.1, it is evident that the vegetation around the Capitol building has not been correctly separated.

340           The errors in classification are surmised to be a result of spectral similarities  
341 among various groups of scene classes, namely -

- 342       • ROAD, ROOF and PATH;
- 343       • WATER and SHADOW; and
- 344       • TREE and GRASS.

345           Other undesirable traits of the output include speckle classifications (such as  
346 isolated identifications of ROOF on roads because of traffic and debris). Since the  
347 multispectral data has been gathered at a high resolution, a visual assessment of the  
348 output is a reliable means to guide analysis. The quantitative assessment of the output is  
349 presented in Section 3.2.12.

350

### 351 **3.2.3 Node 1 - Separating WATER + SHADOW**

352           From the output at the Root Node, Figure 3.4b, it is evident that spectral  
353 separation between WATER and SHADOW can be problematic. This is a result of the  
354 energy absorption by water, which results in a spectral response that is similar (low in  
355 magnitude) to that of a SHADOW region.

356           Though there is confusion in separating WATER from SHADOW, the separation of  
357 these from other classes is accurate, and complete. Thus, the masking scheme of Section  
358 3.1.5 is applicable to pull WATER+SHADOW from the remainder of the data, and is  
359 followed by the binary segmentation discussed in Section 3.1.2 to separate the masked  
360 data into WATER and SHADOW.

361           Several experiments with the above scheme were conducted. In each case, the  
362 separation of classes WATER and SHADOW was not clean (visually). Ultimately, the  
363 resolution of the deficiencies was postponed to a later stage (cf. Section 3.2.9 - Node 8).

364

### 365 **3.2.4 Node 2 - Segmenting SHADOW**

366           In general, SHADOW is a composite of sub-classes comprising various low energy  
367 responses on diverse materials. The objective of this stage was to separate the SHADOW  
368 class into its sub-classes. The data classified as SHADOW in Figure 3.4a were isolated by  
369 the masking process and the binary segmentation algorithm was applied. It was observed  
370 that one of the SHADOW sub-classes generated by the procedure correctly identified



371 water elements in the scene. This corresponded to the discovery of a new scene-class  
372 and was labeled WATER2. The experiment was repeated several times. In each case, the  
373 performance of the operation was mediocre (visual analysis). It was surmised that the  
374 assumption of the unimodal probability distribution for the SHADOW class, as used in the  
375 algorithm for the unsupervised segmentation [7], might be a poor modeling.

376

### 377 **3.2.5 Node 3 - Separating GRASS and TREE**

378 From the output at the Root Node, Figure 3.4e, it is evident that there are  
379 portions of the scene where there is confusion in classifying between GRASS and TREE.  
380 The data for classes TREE and GRASS are masked out from the remainder of the scene  
381 and the binary segmentation algorithm was applied to re-separate the merged classes  
382 into TREE and GRASS.

383 This stage is subsequently referred to as Node 3.

384

### 385 **3.2.6 Node 4 - Extracting rooftops**

386 One of the critical goals of this analysis is the extraction of roofs in the scene<sup>3</sup>.  
387 While the definition of a roof would generally imply "the cover of any building" [11],  
388 such a classification is complicated to implement via spectral analysis. There is an  
389 immense diversity in the materials used in constructing rooftops and in their condition,  
390 and consequently no single spectral response is representative of the class ROOF. At the  
391 Root Node, several spectral sub-classes of ROOF were identified and merged into one  
392 group at the end of the analysis. The elements identified as ROOF in Figure 3.4a can be  
393 masked from the remainder of the data. The masked output is represented as a black and  
394 white image in Figure 3.5.

395 Given multispectral data of the scene it is possible to achieve good separation  
396 between the composite class ROOF and other scene-classes. However, this is contingent  
397 upon the identification of a comprehensive list of ROOF sub-classes, and a well-executed  
398 selection of the respective training data. An alternate means for the analysis is proposed  
399 here based on the Digital Elevation Map (DEM) of the scene.

---

<sup>3</sup> The discussion of this section has also been published elsewhere [12].

400           Each pixel in the DEM is representative of the elevation of the area  
401 corresponding to the pixel on the ground. By definition, the information content of this  
402 data is directly relevant to the identification of rooftops in the scene. A grayscale  
403 representation of the DEM is shown in Figure 3.2. The lighter pixels in the image  
404 correspond to elements at higher elevations in the scene.

405           The DEM provides information on the rise in elevation of a given area-element  
406 in relation to its neighbor. The proposed solution took the following route.

- 407 - It was assumed that all the rooftops in the flightline are contained in the classes  
408 ROAD, PATH, ROOF and SHADOW identified at the Root Node. The first step in the  
409 process was a masking operation on the four classes, excluding the remainder of the  
410 scene in the thematic map (and associated HYDICE data) from subsequent analysis.
- 411 - Rooftop identification followed via a thresholding operation on the elevations of all  
412 data elements identified above. The procedure was designed as a Boolean-type  
413 operation in which all data (identified as one of the four classes listed above) below  
414 a certain elevation were said to be at ground level; the filtered data were thus  
415 identified as building-rooftops.
- 416 - Since there was some amount of variation in scene elevation, the elevation threshold  
417 had to be locally determined. This was accomplished by partitioning the scene into  
418 several zones. The zones were defined as regions of relatively unchanging terrain  
419 elevation and the elevation threshold for each zone was obtained independently. This  
420 scheme is detailed in [12].

421           The result of the ROOF identification operation is shown in Figure 3.6. Data that  
422 had previously been identified with this class, but was not retained after the analysis of  
423 this stage was assigned the class ROOF-RESIDUE.

424

425



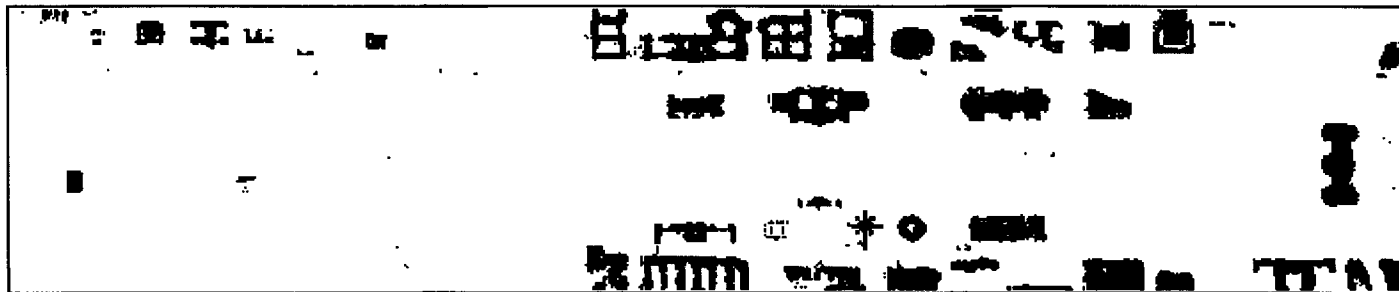
426

427

428

429

Fig. 3.5: Scene class ROOF isolated from the remainder of the thematic map of Figure 3.4a using the masking operation.



430

431

432

433

434

Fig. 3.6: The output of the operation at Node 4 isolates the ROOF class based on a filtering operation on the scene elevations.

435 **3.2.7 Node 5 - Negative training on PATH**

436 It is evident from Figure 3.4 that speckle misclassification compromises the  
437 quality of the output. One way to overcome such errors is to forego the use of the  
438 spectral data completely in subsequent processing. The reason for this proposition is that  
439 spectral information need not necessarily reflect the target objective. For instance,  
440 spectral data on roads is 'corrupted' by presence of cars etc. While the statistical spectral  
441 classification is true to the data, the returned output is likely cluttered with speckle noise.  
442 To counter such problems, the analyst can make the judgment that a given scene-class is  
443 restricted to a certain portion of the scene and perform the "negative training" operation  
444 sketched earlier. In this case, the scene-class PATH was isolated to a small strip restricted  
445 to the center of the flightline for application of the operation, and all other PATH  
446 classifications outside this strip were re-assigned. The analysts based this decision on a  
447 visual inspection of Figures 3.1 and 3.4.

448

449 **3.2.8 Node 6 - Negative training on WATER2, WATER**

450 It was desired to remove all classifications of WATER or WATER2 that are  
451 erroneous from the classification map. It was an analyst decision to restrict  
452 WATER/WATER2 classification spatially, to the three large water bodies that could be  
453 visually identified in Figure 3.1. The Negative Training module could then be used to  
454 clear the remainder of the scene of clutter associated with WATER classification.

455

456 **3.2.9 Node 7 - Re-assigning SHADOW (spectral method)**

457 It has been noted that distinguishing the class SHADOW from the remainder of the  
458 data is a difficult task. The original motive for identifying SHADOW in the data was to  
459 explain the low energy in the spectral readings over various portions of the image.  
460 Failure to do so had resulted in a poor statistical classification of the data. At this stage  
461 however, it was concluded that the class SHADOW was non-informative, and had to be  
462 removed from the set of scene classes. The maximum likelihood classification module  
463 was used to re-assign labels to all data that had been previously classified as SHADOW.  
464 The training data for the module were the remainder of the data in the scene, labeled as  
465 per the classification map at Node 1.

466

467 **3.2.10 Node 8 - Negative training on classes WATER + WATER2**

468 As expected, because of the high spectral similarity (low magnitude of response)  
469 between the class SHADOW and WATER, most of the re-assigned data in Node 7 got  
470 classified as WATER. The negative training operation was applied, as at Node 6, to  
471 remove the occurrences of water classification outside the regions pre-defined by the  
472 analyst as water bodies.

473

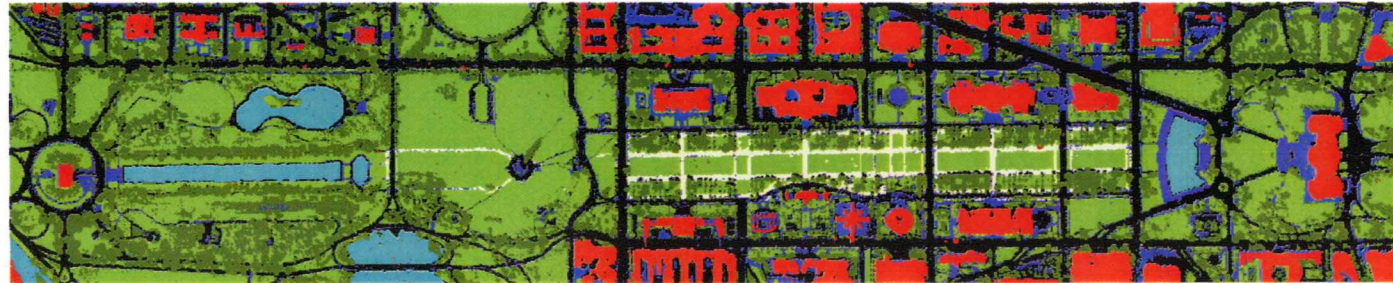
474 **3.2.11 Node 8b - Reassigning class SHADOW (spatial scheme)**

475 Instead of the scheme used at Nodes 7 and 8, it could have been preferred that  
476 the re-assignment of the SHADOW pixels was done via a voting scheme on the labels of  
477 the respective eight point neighborhoods. This technique would have negated the need  
478 for Node 7, the negative training on WATER. It was discovered that the outputs at Nodes  
479 8, 8b were very similar – both by subjective evaluation and by quantitative  
480 measurement. The output in Figure 3.7 corresponds to that obtained at Node 8.

481

482  
483

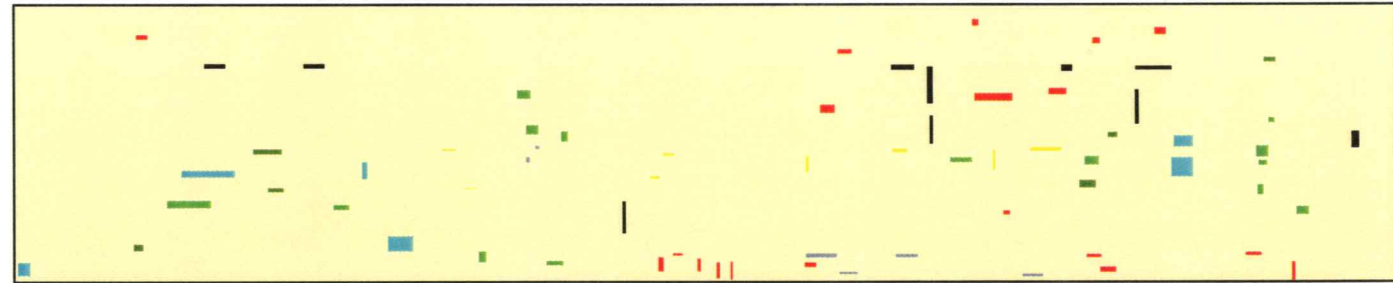
- Groups
- Tree
  - Water
  - Roof
  - Road
  - Path
  - Roof-residue
  - Grass



484  
485  
486  
487  
488

Fig. 3.7: Thematic map generated at Node 8 of the analysis, used as final output.

- Classes
- background
  - Water
  - Road
  - Shadow
  - Path
  - Tree
  - Grass
  - Roof



489  
490  
491  
492  
493

Fig. 3.8: Representation of test data used in assessing performance of classification analysis [13].

494 **3.2.12 Synopsis**

495 The output shown in Figure 3.7 passed the criteria for subjective evaluations –  
 496 absence of clutter, verification by regional expert for absence of logical aberrations in  
 497 classifications. A quantitative assessment of this output was carried out against the test  
 498 data identified in Figure 3.8. These test data were gathered by a researcher [13]  
 499 independent of the analysis presented here, as representative samples of each scene-class  
 500 in the flightline. The output in Figure 3.7 could thus be compared to the samples  
 501 identified in Figure 3.8 to evaluate the accuracy of the analysis. The classification  
 502 performance at Node 8 is tabulated in Table 3.1 for each of the scene-classes. For  
 503 comparison, Table 3.1 also lists the classification performance at the Root Node.

504 Table 3.1: A quantitative assessment of classification outputs at Root Node and Node 8.  
 505  
 506

Scene-class	Number of test samples	Root Node		Node 8	
		Identified number	% accuracy	Identified number	% accuracy
ROAD	1 056	1 018	96.40	1 016	96.21
WATER	1 566	1 456	92.98	1 556	99.36
PATH	261	246	94.25	238	91.19
TREE	450	429	95.33	428	95.11
GRASS	1 378	1 029	74.67	1 270	92.16
ROOF	1 192	974	81.71	1 059	88.84 <sup>4</sup>
All classes	5 903	5 152	87.28	5 622	94.31

507 The analysis procedure can be summarized by the representation shown in  
 508 Figure 3.9. It is implicit that the output at a terminal node in the directed graph is  
 509 retained for the final output without further processing.  
 510

---

<sup>4</sup> The scene-class ROOF, has been characterized in the functional sense in Node 8. If scene-class ROOF-RESIDUE is merged with ROOF, the number of pixels in Node 8 correctly identified as 'roof' is 1 174, and the overall classification accuracy improves to 97.19%.

511  
512

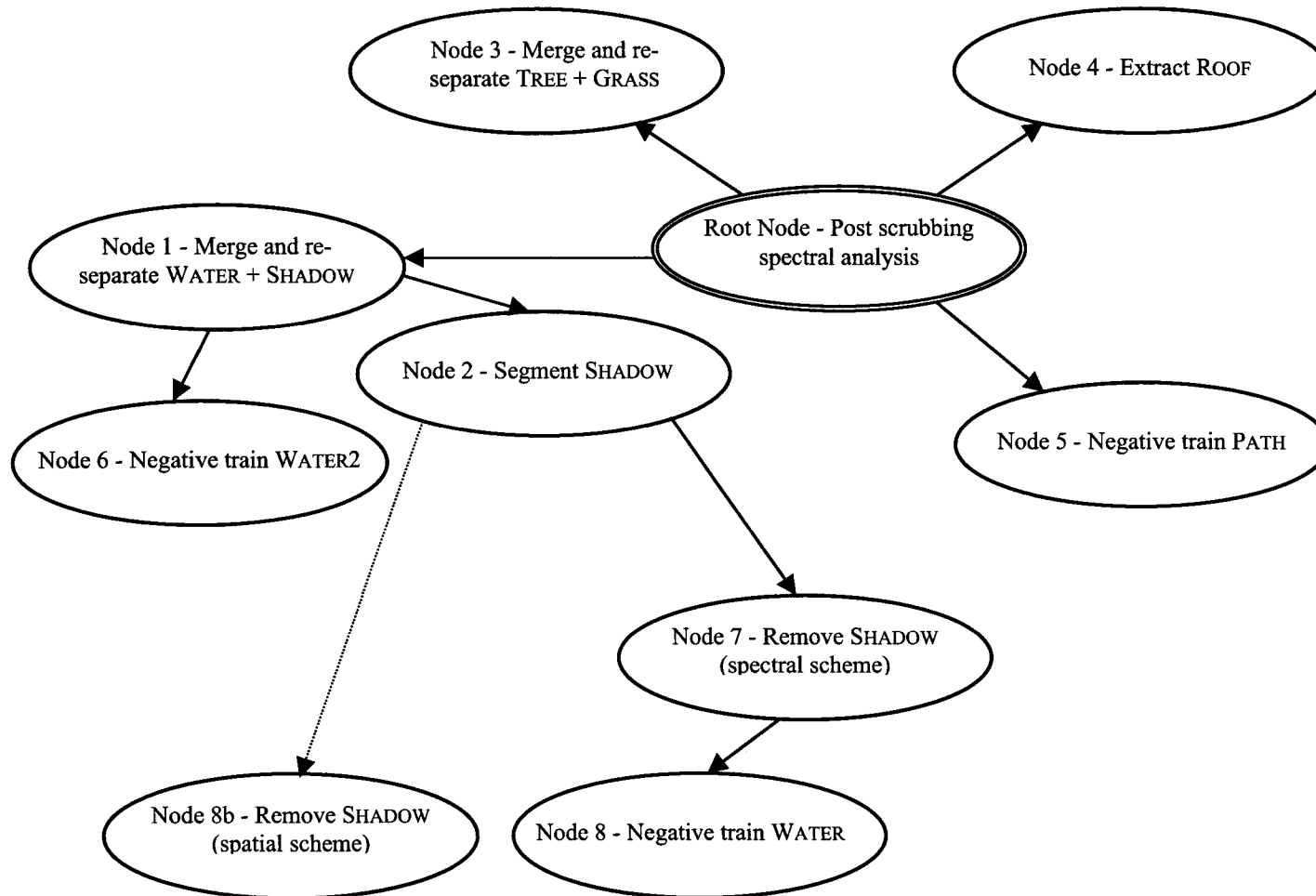


Fig. 3.9: Graph representation of the D.C. data analysis.



513 Some general conclusions of this study are listed below:

- 514 • A hierarchical scheme of analysis can be useful, especially if used to isolate  
515 problematic data for post-processing independent of the remainder of the data.
- 516 • The removal of clutter from the classification output can often be handled without  
517 reliance on the spectral data.
- 518 • When setting the design goals for the analysis, scene-classes can be decided based on  
519 function, or based on composition. For example, in this analysis, the Root Node  
520 identified eight distinct materials used in constructing roofs. However, the goal  
521 focused on the identification of roofs according to usage, and the final output showed  
522 ROOF and ROOF-RESIDUE (the data that were spectrally similar to ROOF, but were  
523 functionally distinct).

524 **4. DISCUSSION**

525 The innate capability for discrimination between very subtle classes by means of  
526 hyperspectral data is very great. However, to achieve this potential with high accuracy  
527 requires a very precise description of the classes desired. This means that, because of the  
528 higher data dimensionality, the size of training sets for the various classes must be large  
529 and must be quite representative of the scene-classes that the analyst has in mind. Thus  
530 one direction to proceed in improving the results obtained at the root node would be to  
531 augment the training sets used. The technique illustrated here provides an alternative to  
532 that procedure in allowing the analyst to achieve an adequately precise version of the  
533 thematic map in mind. Which methodology would be best would depend on the  
534 circumstances of the particular problem.

535 A drawback of the approach presented here is that the methodology for the  
536 solution is not strictly repeatable, since it is unlikely to be as effective, in the exact same  
537 form, in any other project. It can be countered that, while a scientific solution to a given  
538 class of problems seeks robustness and broad applicability, practical concerns demand a  
539 certain level of customization to the solution for every distinct project. It is evident that  
540 the procedure followed in this analysis is not unique. It is a moot point if, and how,  
541 superior results can be obtained using an alternate scheme. Whatever the chosen design,

542 it is believed that the axioms of data fusion proposed in Section 2 and used throughout  
543 the case study of Section 3, would be equally applicable.

544 This study is distinct from several contemporary works in remote sensing research  
545 in that the analysis is conducted as if for an engineering project rather than for an ill-  
546 posed mathematical problem with an uncertain solution. The emphasis is on innovation,  
547 as per the needs of the problem, with procedural guidance obtained from visual  
548 inspection of the output.

## 549 BIBLIOGRAPHY

- 550 [1] D. A. Landgrebe, "Information extraction principles and methods for multispectral  
551 and hyperspectral image data", in *Information Processing for Remote Sensing*, C.  
552 H. Chen, Ed. New Jersey: World Scientific Publishing Co., 2000. Also available  
553 from <http://dynamo.ecn.purdue.edu/~landgreb/publications.html>
- 554 [2] L. Wald, "A European proposal for terms of reference in data fusion", *International*  
555 *Archives of Photogrammetry & Remote Sensing*, vol. XXXII, part 7, pp. 651-654,  
556 1998.
- 557 [3] X. Jia, J. A. Richards, W. Gessner (Editor) and D. E. Ricken (Editor), *Remote*  
558 *Sensing Digital Image Analysis: An Introduction*, 3<sup>rd</sup> ed. Berlin: Springer Verlag,  
559 1999.
- 560 [4] S. D. Kushnier, C. H. Heithecker, J. A. Ballas and D. C. McFarlane, "Situation  
561 assessment through collaborative human-computer interaction", *Naval Engineers*  
562 *Journal*, vol. 108, no. 4, pp. 41-51, July 1996.
- 563 [5] D. M. McKeown, Jr. , S. D. Cochran, S. J. Ford, J. C. McGlone, J. A. Shufelt and  
564 D. A. Yocum, "Fusion of HYDICE hyperspectral data with panchromatic imagery  
565 for cartographic feature extraction", *IEEE Transactions on Geoscience & Remote*  
566 *Sensing*, vol. 37, no. 3, pp. 1261-1277, May 1999.
- 567 [6] B. Schniederman, *Designing the User Interface: Strategies for Effective Human-*  
568 *Computer Interaction*, 2<sup>nd</sup> ed., Reading MA: Addison-Wesley, 1992.
- 569 [7] V. Madhok, "Spectral-spatial analysis of remote sensing data: An image model and  
570 a procedural design", Ph.D. dissertation, School of Electrical and Computer  
571 Engineering, Purdue University, August 1999. Available from  
572 <http://dynamo.ecn.purdue.edu/~landgreb/publications.html>
- 573 [8] L. Biehl, and David Landgrebe, "MultiSpec - A Tool for Multispectral-  
574 Hyperspectral Image Data Analysis", 13th Pecora Symposium, Sioux Falls, SD,  
575 August 20-22, 1996. See also <http://dynamo.ecn.purdue.edu/~biehl/MultiSpec/>

- 576 [9] K. Fukunaga, *Introduction to Statistical Pattern Recognition*, San Diego CA:  
577 Academic Press Inc., 1990.
- 578 [10] C. Lee and D. A. Landgrebe, "Analyzing high-dimensional multispectral data",  
579 *IEEE Transactions on Geoscience & Remote Sensing*, vol. 31, no. 3, pp. 792-800,  
580 July 1993. Also available from  
581 <http://dynamo.ecn.purdue.edu/~landgreb/publications.html>
- 582 [11] *Webster's Ninth New Collegiate Dictionary*, Springfield MA: Merriam-Webster,  
583 1993.
- 584 [12] V. Madhok and D. Landgrebe, "Supplementing Hyperspectral Data with Digital  
585 Elevation", *Proceedings of the International Geoscience & Remote Sensing*  
586 *Symposium (IGARSS)*, June 28 - July 2, 1999. Also available from  
587 <http://dynamo.ecn.purdue.edu/~landgreb/publications.html>
- 588 [13] Y. Zheng, private communication.